Novel Amiodarone−Doxorubicin Cocktail Liposomes Enhance Doxorubicin Retention and Cytotoxicity in DU145 Human Prostate Carcinoma Cells

Theodossis A. Theodossiou,* Maria C. Galanou, and Constantinos M. Paleos

DendriGen A.E., 3 Afxentiou Street, 174 55 Alimos, Athens, Greece

We have developed novel cocktail liposomes bearing doxorubicin in their hydrophilic cores, and amiodarone, a potent multidrug resistance inhibitor, in their lipid bilayers. The efficacy of these liposomes was studied in DU145 human prostate carcinoma cells. Intracellular calcein retention, which is inversely proportional to multidrug resistance activity, significantly increased following cell incubation with amiodarone loaded liposomes. Fluorescence confocal microscopy on cells incubated with the cocktail liposomes revealed enhanced intranuclear doxorubicin accumulation. Two liposomal drug concentration combinations were employed to assess the differential cytotoxicity of the cocktail liposomes, doxorubicin (1.4 μM)−amiodarone (15 μM) and doxorubicin 3 (μM)−amiodarone (45 μM), and two incubation times, 5 and 19 h. Cell toxicity was determined by XTT assays at 24, 48, and 72 h following incubation and was significantly enhanced for incubation with the cocktail liposomes. On the whole, we believe that these liposomes will greatly contribute to the cancer chemotherapy arena.

Introduction

One of the main problems in cancer chemotherapy is the emergence of drug resistant tumor cells, a common phenomenon in patients with advanced tumors.[1,2] This type of resistance collectively known as multidrug resistance (MDR[a]) is probably the main cause of the failure of chemotherapy drug action. The best understood form of MDR in human cells is attributed to P-glycoprotein (Pgp),[3] a member of the ABC superfamily of transporter proteins,[4] which is encoded by the MDR1 gene.[5] Pgp is resident on the plasma membrane and can expel a broad range of internalized anticancer drugs against a concentration gradient.[3,5,6]

Pgp, however, is not the only cause of MDR; many drug resistant cell lines do not exhibit elevated levels of Pgp and yet manage to withstand lethal doses of a wide range of natural product drugs.[7−9] Some of these cell lines express up-regulated levels of a second protein—also member of the ABC superfamily—the MDR associated protein (MRP).[10−13] Much like Pgp, MRP seems to act as a drug efflux pump,[14] is mainly present in the plasma membrane too,[14] and has the ability to diminish intracellular drug levels against a concentration gradient.[14]

A third form of drug resistance associated with several drug types is conferred by increased levels of reduced glutathione (GSH) and/or glutathione *S*-transferase[15−19] occurring in two steps: (a) formation of GSH S-conjugate with the drug and (b) removal of the toxic complex from the cell interior via a GSH S-conjugate export carrier, the GS-X pump,[20] also known as multispecific organic anion transporter (MOAT).[21]

Although the above mechanisms may profoundly increase in tumor cells following repeated treatments with their substrates,[2] they are also inherent in parent cell lines, where MDR defeat leads to elevated cell toxicity.

One of the most prominent chemotherapeutic agents affected by MDR is doxorubicin (DOX), a natural anthracycline glycoside, antineoplastic antibiotic isolated from *Streptomyces peucetius*. Its principle mode of action is through DNA intercalation and inhibition of both DNA and RNA synthesis[22−24] by stabilization of topoisomerase II.[25] Even though conventional DOX has been extensively used in the clinic to combat various forms of cancer, its effectiveness is limited by its low therapeutic index attributed to two main factors: (a) its high toxicity incurring side effects such as myelosuppression, alopecia, acute nausea and vomiting, stomatitis, and cumulative cardiotoxicity[26] and (b) the strong MDR response, implicating all three mechanisms discussed above,[10,27,28] in tumor cells after repeated administration.

Reversal of cancer cell MDR response has been achieved by the coadministration of various MDR inhibitors such as cyclosporine A, verapamil, PSC 833 and amiodarone both in vitro and in vivo.[29−32] Of these inhibitors, amiodarone, originally an antiarrythmic drug, has also been reported to possess anti-inflammatory and antioxidative properties.[33] A pilot clinical study performed with the coadministration of amiodarone and infusional DOX has been performed;[34] however, it was inconclusive with respect to Pgp blocking because of the need of an alternative treatment plan design.

The therapeutic index of DOX has greatly increased following its liposomal encapsulation.

Doxorubicin-loaded liposomes exhibit enhanced efficiency in some forms of cancer in comparison to free drug administration, as liposomes accumulate in the extracellular space of the target tumors through the enhanced permeability and retention effect (EPR),[35,36] resulting in increased drug payloads delivered to the neoplastic formations. EPR is a result of the leaky vascular

[a] Abbreviations: MDR, multidrug resistance; Pgp, P-glycoprotein; GSH, reduced glutathione; MOAT, multispecific organic anion transporter; DOX, doxorubicin; EPR, enhanced permeability and retention effect; DLS, dynamic light scattering; PEG, polyethylene glycol; ODG, octadecylguanidine hydrochloride; FBS, fetal calf serum; calcein AM, calcein acetomethyl ester; XTT, 2,3-bis(2-methoxy-4-nitro-5-sulfophenyl)-2*H*-tetrazolium-5-carboxanilide; DMSO, dimethyl sulfoxide; PC, phosphatidylcholine; CHOL, cholesterol; PBS, phosphate buffer saline; FITC, fluorescein isothiocyanate; ITC, isothermal titration colorimetry.
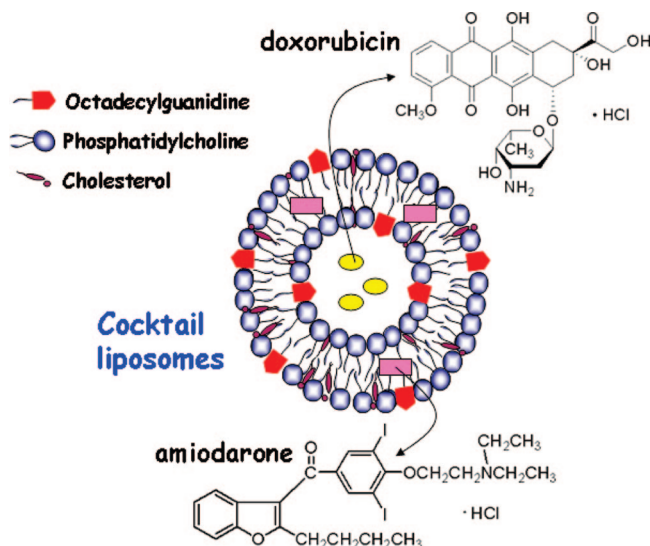
Figure 1. Schematic representation of the cocktail liposomes with DOX encapsulated in their aqueous cores and amiodarone incorporated in their lipid bilayers. The liposomes were further functionalized with guanidinium groups (ODG) on their surfaces to achieve strong binding through molecular recognition with the various anionic groups (phosphate, sulfate, carboxylate, etc.) resident on the cell plasma membranes through molecular recognition.

endothelial linings of growing neoplasias, leaving gaps in the endothelium of up to 800 nm in diameter, large enough to permit the extravasation of liposomes with diameters in the range of 100 nm.[37] Moreover, developing tumors have defective lymphatic drainage, which extends the residence time of extravasated liposomes in the tumor extracellular space, allowing them to gradually release their encapsulated drug and thus exert anticancer effects. One such commercial DOX liposomal formulation is currently approved for use in AIDS-associated Kaposi sarcoma, refractory ovarian cancer, and metastatic breast cancer,[38−42] with the benefit of profoundly reduced DOX-associated cardiotoxicity.

In the present study we developed cocktail liposomes containing DOX in their hydrophilic cores and amiodarone in their lipid bilayers (Figure 1). The reason we chose amiodarone among other MDR inhibitors is its free solubility in chloroform and thus the ability for better incorporation into the liposomal formulations as well as its high potency. Our aim was to test these liposomes and provide proof of principle of their ability to increase DOX intracellular retention and cytotoxicity in DU145 human prostate carcinoma cells.

The external surfaces of these liposomes were additionally functionalized with guanidinium groups (Figure 1) in order to achieve better binding to the cell plasma membranes via combined electrostatic forces and hydrogen bonding[43,44] with various anionic groups located on the outer surface of the cell membrane (phosphate, sulfate carboxylate etc.). This interaction, attributed to molecular recognition, has been previously exploited to achieve more effective cell internalization of macromolecules.[45,46]

Results

Liposome Characterization. The liposomes produced throughout this work were of similar sizes. Their mean hydrodynamic radii as measured by dynamic light scattering (DLS) were found to range from 40 to 55 nm (80−110 nm diameter). The concentrations of encapsulated amiodarone in the lipid bilayer
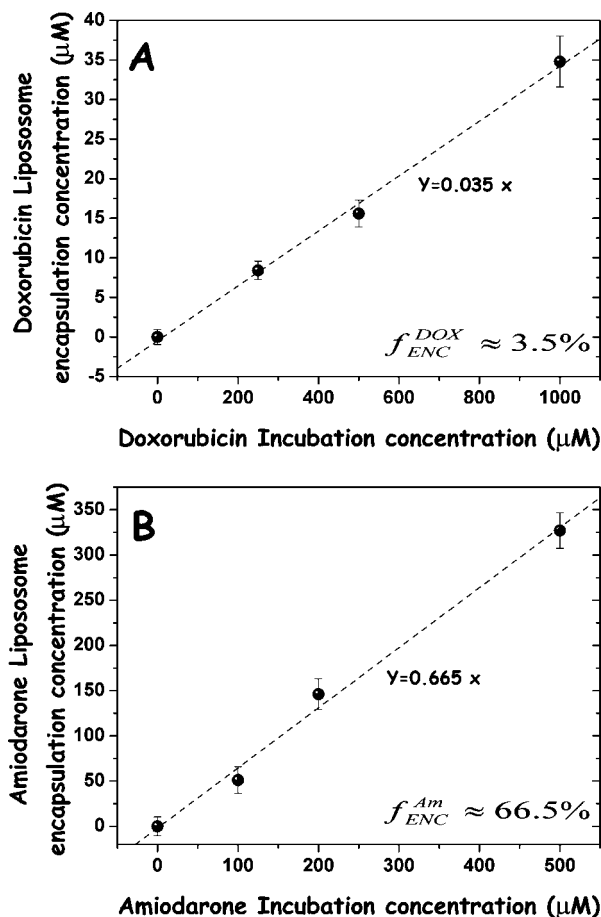

Figure 2. Liposomal encapsulation of (A) doxorubicin and (B) amiodarone. Encapsulation concentrations are expressed as equivalent free drug concentrations in the liposomal dispersion and are plotted against drug concentrations added to the lipid films during liposome preparation. The mean encapsulation fractions are obtained from the slopes of the linear regressions. The error bars represent the standard deviations on the points.

and DOX in the aqueous cores of the liposomes were determined as described in the Experimental Section. A useful parameter regarding drug encapsulation in the liposomes under investigation is the encapsulation fraction

$$f_{\text{ENC}} = \frac{C_{\text{ENC}}}{C_{\text{INC}}} \quad (1)$$

where f_{ENC} is the encapsulation fraction, C_{ENC} is the concentration of the drugs encapsulated in liposomes, and C_{INC} is the concentration of amiodarone or DOX added to the lipid films. The encapsulated DOX and amiodarone concentrations together with their corresponding average encapsulation fractions, as determined from the slopes of the linear fits to the encapsulation vs incubation concentration data points, are shown in Figure 2A and B, respectively. The data therein represent the mean values of all acquired measurements. The average encapsulation fractions for DOX and amiodarone were found to be $f_{\text{ENC}}^{\text{DOX}} \approx$ 3.5% and $f_{\text{ENC}}^{\text{Am}} \approx 66.5\%$, respectively.

Calcein AM Assay. The calcein acetomethyl ester (calcein AM) retention results are summarized in Figure 3. A representative confocal image of a DU145 cell incubated with control liposomes for 4 h and calcein AM during the final (fourth) incubation hour is shown (Figure 3A). The image in Figure 3B is characteristic of a cell incubated with amiodarone loaded liposomes (equivalent incubation concentration of 17 μM). There
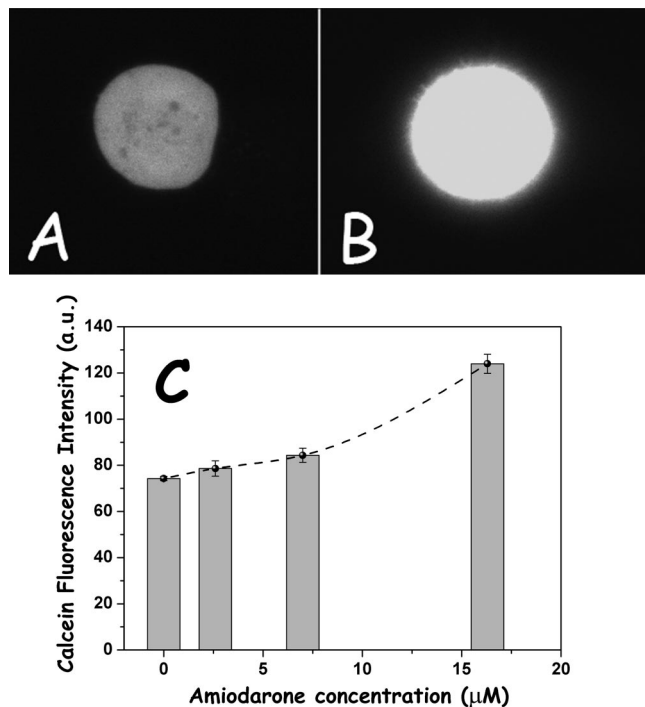
Figure 3. Calcein AM retention studies. (A) Confocal fluorescence microscopy image typical of cells incubated with control (empty) liposomes for 4 h and with 400 nM calcein AM during the fourth hour of incubation. (B) Confocal fluorescence microscopy image representative of cells incubated with amiodarone loaded liposomes (equivalent incubation concentration of 17 μM) for 4 h and with 400 nm calcein AM during the fourth hour of incubation. Calcein fluorescence was excited at 488 nm and imaged through a 522 ($\pm$35) nm dichroic filter for the aqusition of parts A and B. (C) Fluorescence microplate assay. Cells were incubated with control liposomes, as well as with amiodarone loaded liposomes (equivalent free drug concentrations of 0−17 μM) for 1.5 h, while half hour prior to incubation completion, 400 nM calcein was added to all cells. Calcein end point fluorescence was measured at 492 nm excitation and 520 nm emission using a Fluostar Galaxy plate reader.

is a considerable difference in cytosolic calcein fluorescence intensity between the two images. In Figure 3C the results of the microplate fluorometric assay are shown for cells incubated with liposomes of varying amiodarone content (equivalent incubation concentrations of 0−17 μM) for 1.5 h, while an amount of 50 μL of 1 μM calcein AM was added to each well during the final half-hour of incubation. The data show a monotonic increase in calcein fluorescence for increasing liposomal amiodarone concentrations.

Liposomal Amiodarone−DOX Confocal Microscopy. Typical images of cells incubated with DOX loaded liposomes (equivalent incubation concentration of 3 μM) for 4 h are shown in Figure 4A (zoom 1) and Figure 4C (zoom 2). The confocal images in parts B and D of Figure 4 are representative of cells incubated with DOX−amiodarone loaded liposomes (equivalent incubation concentrations of 3 and 45 μM, respectively) for 4 h (zooms 1 and 2 in that order). Apart from the significant increase in overall DOX fluorescence intensity in parts B and D of Figure 4, there is also a marked enhancement of the intranuclear fluorescence intensity. In the presence of amiodarone, DOX seems to be able to accumulate in the cell nuclei, its intended site of action, more efficiently. Images of cells incubated with control liposomes were also registered; however, there was no apparent fluorescence (data not shown).

Liposomal Amiodarone−DOX Cytotoxicity. Cytotoxicity results on cell groups incubated with liposomes loaded with
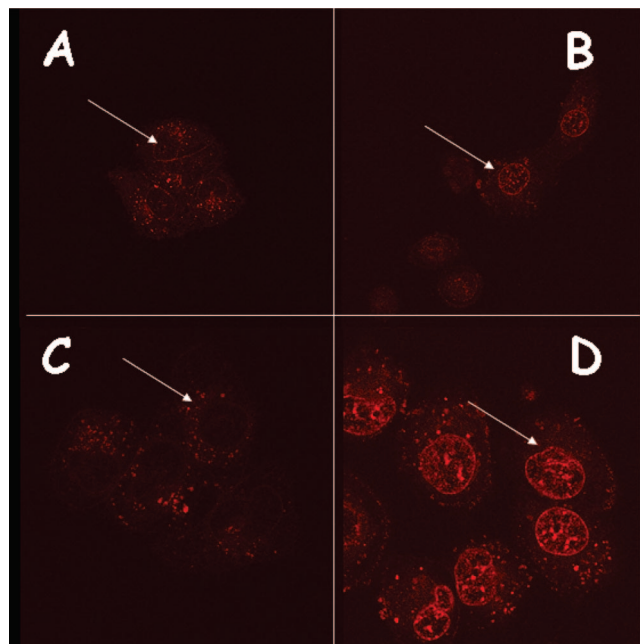

Figure 4. DOX fluorescence cell confocal images: (A, C) cells incubated with DOX loaded liposomes (equivalent free drug concentration 3 μM) for 4 h, zooms 1 and 2, respectively; (B, D) cells incubated with DOX-amiodarone loaded liposomes (equivalent incubation concentrations of 3 and 45 μM, correspondingly) for 4 h, zooms 1 and 2, respectively. The presence of amiodarone in the liposomes incurred enhanced accumulation of DOX in the cell nuclei (white arrows). DOX fluorescence was excited at 488 nm and imaged through a 585 nm dichroic filter (585 EFLP). A three-step Kalman smoothing filter was in all cases applied for image acquisition.

DOX, amiodarone, or DOX and amiodarone for 5 h and 19 h incubation as assayed by 2,3-bis(2-methoxy-4-nitro-5-sulfophenyl)-2H-tetrazolium-5-carboxanilide (XTT) at 24, 48, and 72 h following incubation are presented in Figures 5 and 6. These cytotoxicity results of DOX and DOX amiodarone liposomes are replotted as a function of the assay time in the linear graphs of parts A and B of Figure 7 to provide an alternative perspective. In Figure 7A the lower DOX−amiodarone concentrations are presented, whereas the higher DOX−amiodarone concentrations are shown in Figure 7B.

The data in Figures 5 and 7A, were obtained using liposomes bearing DOX in their cores (equivalent free drug concentration of 1.4 μM), amiodarone in their lipid bilayers (equivalent free drug concentration of 15 μM), or DOX and amiodarone (equivalent incubation concentrations 1.4 and 15 μM, respectively). From Figure 5A, which depicts cytotoxicity 24 h following incubation, it can be deduced that amiodarone conferred minimal cytotoxicity for 5 and 19 h of incubation (10−15%), whereas DOX alone conferred approximately 30% cytotoxicity for both incubation regimes. Incubation with liposomes bearing both DOX and amiodarone conferred >40% cytotoxicity, which was statistically significant compared to the DOX alone values ($p = 0.0002$ for 5 h and $p = 6 \times 10^{-5}$ for 19 h of incubation by Student paired t tests). The toxicity for the 19 h incubation groups increases at 48 h following incubation. Again comparison between the DOX alone and DOX amiodarone groups shows statistical significance, although somewhat reduced for 5 h of incubation ($p = 0.004$ for 5 h and $p = 10^{-6}$ for 19 h of incubation). XTT assays at 72 h following incubation reveal further enhancement of toxicity for both 5 and 19 h incubations. The values for the 5 h incubation between the DOX alone and amiodarone−DOX groups are not statisti-
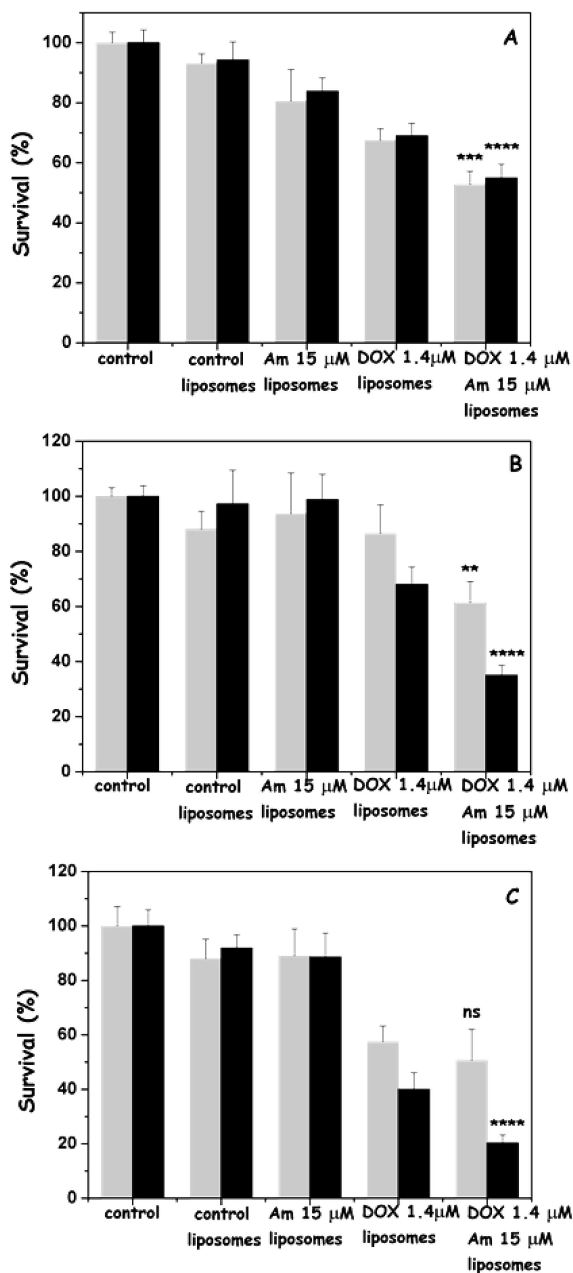
Figure 5. Liposomal DOX cytotoxicity on DU145 cells with/without amiodarone encapsulated in the liposome lipid bilayer (equivalent free drug concentrations of 1.4 μM for DOX and 15 μM for amiodarone). The toxicity was determined by a standard XTT assay performed at 24 (A), 48 (B), and 72 h (C) following incubation. Two incubation times were studied: 5 h (light-gray columns) and 19 h (black columns). Student paired *t* tests were performed between the cell groups incubated with DOX and amiodarone−DOX liposomes in all cases: (ns) $p > 0.05$; (∗) $p < 0.05$, (∗∗) $p < 0.01$; (∗∗∗) $p < 0.001$; (∗∗∗∗) $p < 0.0001$.

Figure 6. Liposomal DOX cytotoxicity on DU145 cells with/without amiodarone encapsulated in the liposome lipid bilayer (equivalent incubation concentrations of 3 μM for DOX and 45 μM for amiodarone). The toxicity was determined by a standard XTT assay performed at 24 (A), 48 (b), and 72 h (C) following incubation. Two incubation times were studied: 5 h (light-gray columns) and 19 h (black columns). Student paired *t* tests were performed between the cell groups incubated with DOX and amiodarone−DOX liposomes in all cases: (∗∗∗∗) $p < 0.0001$.

cally different this time ($p = 0.1$), while for the 19 h incubation there is enhanced cytotoxicity in the amiodarone−DOX group ($p = 3 \times 10^{-7}$). We repeated the cytotoxicity investigations for increased DOX and amiodarone liposomal encapsulation (equivalent free drug concentrations of 3 and 45 μM, respectively). The results are summarized in Figures 6 and 7B. The toxicity assay at 24 h revealed minimal cell death following incubation with amiodarone liposomes for 5 h and approximately 30−40% toxicity (DOX liposomes) for 19 h of incubation. The respective values of DOX toxicity were about 20%, while the cytotoxicity of cocktail liposomes was largely
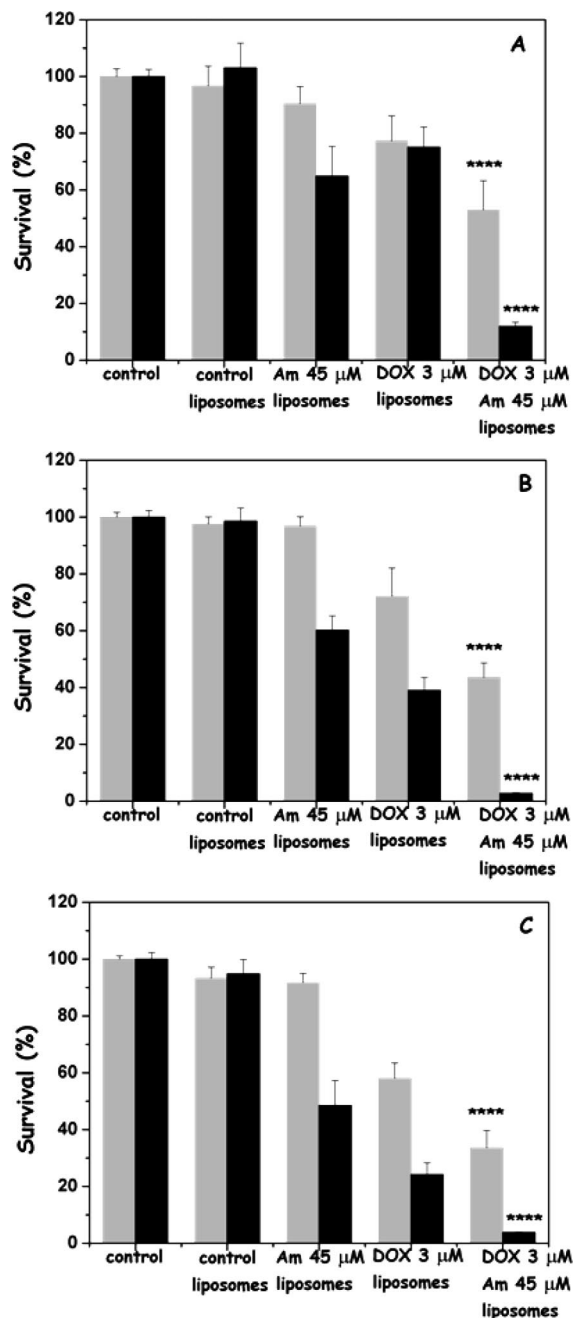
increased (∼55% for 5 h of incubation and ∼80% for 19 h of incubation). Comparison between the DOX and amiodarone−DOX groups showed statistically significant enhancement of cytotoxicity in the case of cocktail liposomes for both 5 and 19 h of incubation ($p = 4 \times 10^{-5}$ and $p = 8.5 \times 10^{-10}$, respectively). The toxicity was enhanced 48 h following incubation, and profound differential toxicity of the amiodarone−DOX groups was observed ($p = 8.5 \times 10^{-5}$ for 5 h and $p = 2 \times 10^{-8}$ for 19 h of incubation). The cocktail liposome treatment for 19 h caused approximately 97% cell death. The toxicity
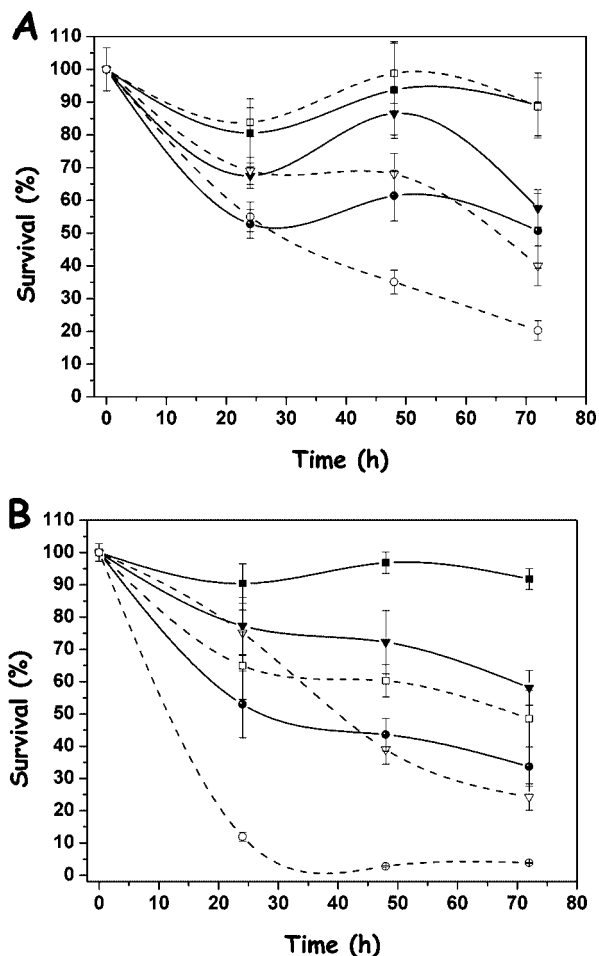
Figure 8. Schematic representation of the ODG lipid inserted into the liposomal lipid bilayer.

further increase the therapeutic index of DOX via defeat of MDR mechanisms. This research was triggered by the well documented synergistic effects of parallel administration of nonliposomal DOX and amiodarone in vitro and in vivo.[30−32,34]

Even though existing clinical doxorubicin formulations employ PEGylated liposomes to evade opsonization and thus prolong liposome circulation in vivo, the present study was performed entirely in vitro; therefore, there was no need to circumvent any immune response and consequently we did not need to introduce the extra parameter of liposome PEGylation at this stage. Although one might argue that PEGylation could hinder molecular recognition between the liposomal guanidinium moieties and plasma membrane anionic groups, our previous data show that this shielding still allows the above interaction.[47,48] Moreover, our group is currently exploring the possibility of incorporating the guanidinium group at the distal end of liposomal PEG chains, and the initial results show enhanced interaction in comparison to surface guanidinylation.

We conducted our experiments on a parent DU145 human prostate carcinoma cell line to evaluate the potential efficacy of our cocktail liposomes in a prostate cancer model. It is well established that MDR resistant cell lines derived from repeated administration of a chemotherapeutic agent to their parent cell lines exhibit an enhanced MDR phenotype. For example, repeated exposure to chemotherapy significantly increases the expression of Pgp via the MDR1 gene;[2] however, parent cells also possess MDR mechanisms and defeat of these mechanisms is evident through the differential increase of cell death.

In the present work DOX was encapsulated in liposomes by a passive core encapsulation method through hydration of the films prior to liposome extrusion. The DOX encapsulation yield, although as a percentage is quite low (∼3.5%), was sufficient to confer the cytotoxic effects required (Figures 4 and 5). However, should a higher encapsulation yield be desirable, there are other active loading techniques such as, for example, the pH gradient technique. On the other hand, amiodarone encapsulation was very efficient because amiodarone localized in the liposome lipid bilayer and was directly mixed with the lipids during lipid film preparation, allowing small losses. It is very difficult to comment on the clinical relevance of the amount of drugs entrapped in the liposomes at this stage; further in vitro and in vivo studies are required, as the main aim of the present work was to establish proof of principal of the efficacy of the proposed liposomes. Although commercial formulations may seem to provide a rough guideline, our liposomal formulations are substantially different. One extra factor, for example, that enhanced DOX and amiodarone transfer to the cells from our liposomal preparations was the insertion of the guanidinium bearing octadecylguanidine hydrochloride (ODG) lipid (cartoon Figure 8) into the liposomal lipid bilayer with the guanidinium group protruding from the liposome membrane. The guanidinium group can in this manner strongly bind via combined electrostatic and hydrogen bonding forces[43,44] to the available

Figure 7. Alternative representation: liposomal DOX cytotoxicity on DU145 cells with/without amiodarone encapsulated in the liposome lipid bilayer versus incubation time. The toxicity was determined by standard XTT assays performed at 24, 48, and 72 h following incubation. Two incubation times were studied: 5 h (solid lines, filled symbols) and 19 h (dashed lines, open symbols): (■, □) amiodarone-only liposomes; (▼, ▽) DOX-only liposomes; (●, ○) DOX−amiodarone cocktail liposomes; (A) low dose, equivalent free drug concentrations of 1.4 μM for DOX and 15 μM for amiodarone; (B) high dose, equivalent incubation concentrations of 3 μM for DOX and 45 μM for amiodarone.

values further increased 72 h following incubation for all groups apart for the 19 h incubation cocktail liposome group where cell death was already maximal after 48 h incubation (complete cell death within experimental errors). Again, differential cytotoxic action appeared significantly distinct for the amiodarone−DOX group ($p = 8.5 \times 10^{-9}$ for 5 h and $p = 9.4 \times 10^{-8}$ for 19 h of incubation).

As a whole, the above results suggest a profound enhancement in DOX cytotoxicity by use of cocktail DOX−amiodarone liposomes and especially for longer times of incubation (19 h).

Discussion

Commercially available liposomal DOX formulations are clinically approved for a multitude of ailments such as AIDS associated Kaposi sarcoma, refractory ovarian cancer, and metastatic breast cancer,[38−42] greatly enhancing the therapeutic index of DOX through the EPR effect[35−37] and alleviating DOX associated side effects such as collateral cardiotoxicity.[42] The present work aimed to assess the in vitro efficacy of novel cocktail liposomes bearing DOX in their aqueous centers and amiodarone, a potent MDR inhibitor in their lipid bilayers, to
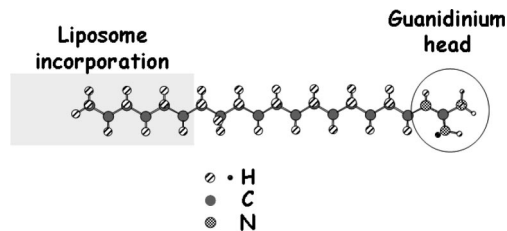
anionic groups that exist in abundance on the outer cell membrane and thus enhance the probability of liposome internalization by the cell. This effect was substantiated in our previous study,[49] where hypericin, a hydrophobic pigment, was encapsulated in ODG–liposomes lipid bilayers. Through a comparison to plain phosphatidicholine–cholesterol liposomes, hypericin transfer to cells was found to increase when ODG–liposomes were employed. Furthermore, in the same study it was shown that lipophilic hypericin encapsulated in the lipid bilayer of guanidinylated liposomes was transferred mainly to the cell membrane while water-soluble (poly-vinyl-pyrolidone) hypericin entrapped in the core of identical liposomes was internalized by the cell. This is very expedient for the cocktail liposomes presented and studied herein; amiodarone encapsulated in their lipid bilayers is expected to be transferred to the cell membrane where it can effectively block the resident MDR proteins while DOX (encapsulated in the liposomal cores) is expected to be transferred to the cell interior where it can ultimately enter the nucleus and exert its action.

The initial calcein AM experiments, performed herein, offered a preview of the ability of amiodarone bearing liposomes to block MDR cell efflux mechanisms. Although the microplate fluorescence technique and confocal imaging concur in support of this conclusion, their results are not directly comparable because of the different experimental conditions and predominantly the prolonged incubation time in the case of confocal imaging. Direct DOX fluorescence confocal imaging of cells incubated with DOX and DOX–amiodarone liposomes further verified the loss of DOX through MDR related efflux from the cells and the inhibitory role of liposomal amiodarone on this extrusion. This phenomenon was manifested both quantitatively, as DOX fluorescence significantly increased in cells treated with DOX–amiodarone liposomes, where MDR mechanisms were subjugated, and qualitatively, as in these cells there was a significant enhancement of DOX accumulation in their nuclei as evident from images B and D of Figure 4.

The increased cytotoxicity of cocktail amiodarone–DOX liposomes, as evident from the data presented in Figures 5–7, is consistent with previous work where free DOX and amiodarone were coadministered to cells.[30-32] In the work presented here, toxicity was amiodarone and DOX dose dependent and was in all cases greater for the 19 h incubation. Although in higher doses of amiodarone there was some amiodarone associated toxicity, this does not seem to account for the levels of death conferred by the DOX–amiodarone liposomes. For example, in the 48 h time frame of cell survival, amiodarone liposomes (45 μM equivalent free drug concentration) resulted in 60% cell survival following 19 h of incubation. The respective values for DOX liposomes and DOX–amiodarone liposomes were 39% and 3%. So a combined amiodarone and DOX effect (0.60 × 0.39 = 0.23, i.e., 23%) is not comparable to the overwhelming effect of the cocktail DOX–amiodarone liposomes (3%).

The benefits from a cocktail liposome (MDR blocker–chemotherapeutic drug) are obvious. Defeat of MDR mechanisms can lead to a better eradication of the target lesion and can also help reduce the chemotherapeutic drug content of the liposomes and retain or even increase the therapeutic effects with the administration of one combinatory medication to the patient. In the case of amiodarone–DOX liposomes, there are already DOX liposomal formulations commercially available and ap-

proved, so the basis already exists while amiodarone is also clinically approved as an antiarrythmic drug.

Experimental Section

Chemicals and Reagents. Soybean hydrogenated phosphatidyl-choline, (Phospholipon 90H, PC) was purchased from Nattermann Phospholipid GmbH. Nucleopore filters of 100 nm pore size (Whatman GmbH, Dassel, Germany) were employed for liposome extrusion. ODG was prepared by the method reported in our previous study.[47] RPMI 1640, fetal bovine serum (FBS), penicillin/streptomycin, L-glutamine, phosphate buffer saline (PBS), trypsin/versene, and calcein AM were purchased from Invitrogen Ltd., (Paisley, U.K.). XTT, cholesterol, methanol, amiodarone, doxorubicin, chloroform, dimethyl sulfoxide (DMSO), and Sephadex G-50 were purchased from Sigma-Aldrich Ltd., Poole, U.K.

Cell Culture. Cells used in this study were the human prostate carcinoma cell line DU145, courtesy of the Urology Scientific Research Department, Division of Surgery, University College London. The cells were grown in RPMI 1640 with 10% FBS, penicillin/streptomycin at 37 °C in a 5% CO_2 humidified atmosphere. Cells were inoculated into either 96-well plates (3×10^4 cells/100 μL media/well) or 35 mm diameter dishes (0.5×10^5 cells/2 mL media /dish) 24 h before experiments.

Preparation of Liposomes. Unilamellar liposomes of approximately 100 nm diameter were prepared by the extrusion method[50] employing a laboratory extruder (LiposoFast-Pneumatic, Avestin Inc.). In a typical experiment for preparing 4 mL dispersion of liposomes, 0.076 mmol (3.8×10^{-2} M) of PC, 0.038 mmol of CHOL (1.9×10^{-2} M) (molar ratio PC/CHOL 2:1), and 0.0058 mmol (1.45×10^{-3} M) ODG were dissolved in chloroform/methanol (2:1 v/v) for the formation, in the usual manner, of lipid films. For the preparation of unilamellar liposomes containing amiodarone in their lipid bilayer, amiodarone was also added to the solution in 100, 200, 500, and 1000 μM final concentrations. The lipid film was hydrated with 4 mL of PBS buffer (pH 7.4), and the sample was vortexed for 10 min at approximately 60 °C. The suspension obtained was extruded through two-stacked polycarbonate filters of 100 nm pore size. Twenty-seven cycles were applied at 60 °C. The encapsulated amiodarone concentration was determined by absorbance (vide infra). Encapsulation of DOX into the liposomal core was performed during hydration of the lipid films with 4 mL of PBS containing DOX in 250, 500, and 1000 μM final concentrations. Removal of nonencapsulated DOX was achieved by size exclusion chromatography (Sephadex G-50). The elution was performed with PBS. The encapsulated DOX concentration was determined by fluorescence spectroscopy (vide infra). The DOX–amiodarone containing liposomal dispersions were diluted appropriately and filter-sterilized through 0.22 μm cellulose acetate filters (Whatman GmbH, Dassel, Germany) prior to cell application.

Liposome Size Characterization. Liposomes were characterized by DLS. For the size determination of liposomes, an AXIOS-150/EX (Triton Hellas) with a 30 mW He–Ne laser emitting at 658 nm and an avalanche detector at right angles were employed. Ten microliters of liposomal dispersion were each time diluted to 0.99 mL of PBS. Ten measurements were collected per sample, and the results were averaged. Further characterization of the liposomes (e.g., ζ-potential measurements) was regarded as redundant, as it has been extensively performed on similar liposomes in a previous study.[51] Furthermore, in that same study, the significantly enhanced interaction between liposomes bearing guanidinium groups and their counterparts bearing phosphate groups was established mainly by isothermal titration calorimetry (ITC).[51]

Amiodarone Encapsulation Determination. For the determination of amiodarone encapsulated in liposome lipid bilayers, a calibration absorbance curve of various amiodarone concentrations (0–50 μM) in methanol containing an amount of lipids and chloroform equivalent to that of 60 μL of liposome dispersion was constructed using a Cary 100 CONC UV–visible spectrophotometer (Varian Inc.) by each time registering absorbance at 240 nm. Aliquots (60 μL) of undetermined amiodarone encapsulation

liposome dispersions were diluted to 3 mL of methanol to ensure complete liposomal membrane disruption and amiodarone release. The absorbance at 240 nm was registered at the same conditions applied to the calibration curve measurements, and amiodarone concentration was each time extrapolated by fitting to the calibration curve.

DOX Encapsulation Determination. For the determination of DOX encapsulated in liposome hydrophilic cores the same procedure as with amiodarone was applied, employing, however, fluorescence instead of absorbance. A calibration curve for various DOX concentrations (0−10 μM) was constructed using a Cary Eclipse fluorescence spectrophotometer (Varian Inc.), each time registering fluorescence intensity at 585 nm, following 490 nm excitation. DOX liposome encapsulation concentrations were each time extrapolated as per the protocol described for amiodarone (vide supra), adapted to the fluorimetric settings.

Calcein AM Assay. The effect of liposomal amiodarone on the multidrug resistance of DU145 cells was initially assayed using calcein AM as a substrate for Pgp efflux activity. In short, calcein AM is a nonfluorescent lipid soluble dye with the ability to rapidly permeate cellular plasma membranes. Once inside the cells the ester bonds are cleaved by endogenous esterases, transforming calcein AM into hydrophilic and intensely fluorescent calcein. MDR mechanisms extrude calcein AM from the plasma membrane, reducing cytosolic accumulation of fluorescent calcein, while upon MDR defeat, calcein is well retained in the cytoplasm.

The assay was performed in two modes: (a) fluorescence microplate and (b) live cell laser scanning confocal fluorescence microscopy imaging.

(a) The fluorescence microplate assay applied was based on the method proposed by Tiberghien and Loor.[52] Cells were inoculated into 96-well plates ((3 × 10^4 cells/100 μL media)/well) and left for 24 h prior to the experiments. Liposomal dispersions with encapsulated amiodarone in equivalent free drug concentrations ranging from 0 (control) to 17 μM were added to the cells and left to incubate for 1 h. Calcein AM, 1 mM, was subsequently diluted to 1 μM in PBS, and an amount of 50 μL of the calcein AM solution was added to each well. The cells were thus incubated for an additional half hour, and subsequently all cell media were removed. Cells were washed twice with PBS, and complete media were added. Fluorescence end point measurements were performed in a Fluostar Galaxy plate reader (BMG Labtechnologies) with the excitation wavelength set to 492 nm and emission set to 520 nm.

(b) DU145 cells were seeded on 22 mm glass coverslips in 35 mm dishes (0.5 × 10^5 cells per dish) and grown overnight. Liposomal dispersions with encapsulated amiodarone (free drug equivalent concentration of 17 μM) were added to the cells and left to incubate for 4 h. Control cells were correspondingly incubated with liposomes devoid of amiodarone. One hour prior to the end of 4 h of incubation, calcein AM in the same concentration as for the microplate assay was added to the cells. Upon incubation completion, the coverslips were twice washed with PBS and placed over the 63× oil immersion quartz objective (NA 1.3) of a Biorad MRC 1024 scanning confocal microscope, in physiological saline. Intracellular calcein was excited using the 488 nm line of an argon−krypton laser (3% of total laser power). Calcein AM fluorescence was collected with the use of a FITC-type dichroic filter centered at 522 (±35) nm. During image acquisition a Kalman level 3 (three iterations per image) smoothing routine was each time applied to eliminate spurious signals.

Amiodarone−DOX Confocal Microscopy. Cells were prepared for confocal microscopy as above. On the day of the experiment, three cell groups were incubated for 4 h with (i) control liposomes, (ii) liposomes with DOX encapsulated in their cores (equivalent DOX incubation concentration of ∼3 μM), and (iii) liposomes with amiodarone encapsulated in their lipid bilayers and DOX in their aqueous centers (equivalent incubation concentrations of ∼3 μM for DOX and ∼45 μM for amiodarone). The cells were in all cases imaged live, without fixing, with the 63× oil immersion quartz objective of the same confocal system as used for calcein imaging, in physiological saline. Excitation was facilitated by the 488 nm

line of an argon−krypton laser (3% of total laser power), while DOX fluorescence was collected with the use of a dichroic filter centered at 585 nm (585 EFLP). Once again, during image acquisition a Kalman level 3 (three iterations per image) smoothing filter was each time applied to eliminate spurious signals.

Cytotoxicity Assessment. Cells grown for 24 h in 96-well plates, as explained earlier, were incubated with media only, control liposomes, amiodarone liposomes (15 and 45 μM equivalent free drug concentrations), DOX liposomes (1.4 and 3 μM equivalent free drug concentrations), and DOX−amiodarone liposomes (1.4−15 and 3−45 μM equivalent concentrations, respectively). These cell groups were subdivided into two groups that underwent 5 and 19 h incubation, respectively, in each occasion. Upon incubation completion, cells were twice washed with PBS and all media were changed to fresh complete media with no liposome content. Mitochondrial redox function (in our case translating directly to cytotoxicity) was assessed in all cell groups at 24, 48, and 72 h following incubation via a standard XTT assay. This relies on the reduction of the tetrazolium salt to a formazan formation by mitochondrial matrix reductive enzymes. In nonredox competent mitochondria, e.g., uncoupled mitochondria or dead cells, no formazan formation occurs. The assay was carried out by adding 150 μL of complete media containing 50 μL of XTT salts (1 mg/mL) and 1 μL of phenazine methosulfate (0.383 mg/ml) to cells and incubating at 37 °C in a 5% CO_2 atm for 2 h. The end point colorimetry was performed at 492 nm in a Fluostar Galaxy plate reader (BMG Labtechnologies). Blank values measured in wells with no cells were subtracted.

Statistics. All experiments were repeated at least three times independently. Cytotoxicity data are shown as the mean, and the errors on graphs represent 1 standard deviation for at least four independent values. Student paired t tests were performed in the cytotoxicity data obtained from cell groups incubated with DOX and DOX−amiodarone.

References

(1) Pastan, I.; Gottesman, M. Multiple-drug resistance in human cancer. *N. Engl. J. Med.* **1987**, *316*, 1388–1393.

(2) Gottesman, M. M. How cancer cells evade chemotherapy: sixteenth Richard and Hinda Rosenthal Foundation Award Lecture. *Cancer Res.* **1993**, *53*, 747–754.

(3) Juliano, R. L.; Ling, V. A surface glycoprotein modulating drug permeability in Chinese hamster ovary cell mutants. *Biochim. Biophys. Acta* **1976**, *455*, 152–162.

(4) Higgins, C. F. ABC transporters: from microorganisms to man. *Annu. Rev. Cell Biol.* **1992**, *8*, 67–113.

(5) Gottesman, M. M.; Pastan, I. Biochemistry of multidrug resistance mediated by the multidrug transporter. *Annu. Rev. Biochem.* **1993**, *62*, 385–427.

(6) Schinkel, A. H.; Borst, P. Multidrug resistance mediated by P-glycoproteins. *Semin. Cancer Biol.* **1991**, *2*, 213–226.

(7) Baas, F.; Jongsma, A. P.; Broxterman, H. J.; Arceci, R. J.; Housman, D.; Scheffer, G. L.; Riethorst, A.; van Groenigen, M.; Nieuwint, A. W.; Joenje, H. Non-P-glycoprotein mediated mechanism for multidrug resistance precedes P-glycoprotein expression during in vitro selection for doxorubicin resistance in a human lung cancer cell line. *Cancer Res.* **1990**, *50*, 5392–5398.

(8) Mirski, S. E.; Gerlach, J. H.; Cole, S. P. Multidrug resistance in a human small cell lung cancer cell line selected in adriamycin. *Cancer Res.* **1987**, *47*, 2594–2598.

(9) Zijlstra, J. G.; de Vries, E. G.; Mulder, N. H. Multifactorial drug resistance in an adriamycin-resistant human small cell lung carcinoma cell line. *Cancer Res.* **1987**, *47*, 1780–1784.

(10) Cole, S. P.; Bhardwaj, G.; Gerlach, J. H.; Mackie, J. E.; Grant, C. E.; Almquist, K. C.; Stewart, A. J.; Kurz, E. U.; Duncan, A. M.; Deeley, R. G. Overexpression of a transporter gene in a multidrug-resistant human lung cancer cell line. *Science* **1992**, *258*, 1650–1654.

(11) Barrand, M. A.; Heppell-Parton, A. C.; Wright, K. A.; Rabbitts, P. H.; Twentyman, P. R. A 190-kilodalton protein overexpressed in non-P-glycoprotein-containing multidrug-resistant cells and its relationship to the MRP gene. *J. Natl. Cancer Inst.* **1994**, *86*, 110–117.

(12) Krishnamachary, N.; Center, M. S. The MRP gene associated with a non-P-glycoprotein multidrug resistance encodes a 190-kDa membrane bound glycoprotein. *Cancer Res.* **1993**, *53*, 3658–3661.

(13) Zaman, G. J.; Versantvoort, C. H.; Smit, J. J.; Eijdems, E. W.; de Haas, M.; Smith, A. J.; Broxterman, H. J.; Mulder, N. H.; de Vries,

E. G.; Baas, F.; et al. Analysis of the expression of MRP, the gene for a new putative transmembrane drug transporter, in human multidrug resistant lung cancer cell lines. *Cancer Res.* **1993**, *53*, 1747–1750.

(14) Zaman, G. J.; Flens, M. J.; van Leusden, M. R.; de Haas, M.; Mulder, H. S.; Lankelma, J.; Pinedo, H. M.; Scheper, R. J.; Baas, F.; Broxterman, H. J.; et al. The human multidrug resistance-associated protein MRP is a plasma membrane drug-efflux pump. *Proc. Natl. Acad. Sci. U.S.A.* **1994**, *91*, 8822–8826.

(15) Leyland-Jones, B. R.; Townsend, A. J.; Tu, C. P.; Cowan, K. H.; Goldsmith, M. E. Antineoplastic drug sensitivity of human MCF-7 breast cancer cells stably transfected with a human alpha class glutathione *S*-transferase gene. *Cancer Res.* **1991**, *51*, 587–594.

(16) Black, S. M.; Beggs, J. D.; Hayes, J. D.; Bartoszek, A.; Muramatsu, M.; Sakai, M.; Wolf, C. R. Expression of human glutathione *S*-transferases in *Saccharomyces cerevisiae* confers resistance to the anticancer drugs adriamycin and chlorambucil. *Biochem. J.* **1990**, *268*, 309–315.

(17) Morrow, C. S.; Cowan, K. H. Glutathione *S*-transferases and drug resistance. *Cancer Cells* **1990**, *2*, 15–22.

(18) Puchalski, R. B.; Fahl, W. E. Expression of recombinant glutathione *S*-transferase pi, Ya, or Yb1 confers resistance to alkylating agents. *Proc. Natl. Acad. Sci. U.S.A.* **1990**, *87*, 2443–2447.

(19) Kramer, R. A.; Zakher, J.; Kim, G. Role of the glutathione redox cycle in acquired and de novo multidrug resistance. *Science* **1988**, *241*, 694–697.

(20) Ishikawa, T. The ATP-dependent glutathione *S*-conjugate export pump. *Trends Biochem. Sci.* **1992**, *17*, 463–468.

(21) Heijn, M.; Oude Elferink, R. P.; Jansen, P. L. ATP-dependent multispecific organic anion transport system in rat erythrocyte membrane vesicles. *Am. J. Physiol.* **1992**, *262*, C104–C110.

(22) Kim, S. H.; Kim, J. H. Lethal effect of adriamycin on the division cycle of HeLa cells. *Cancer Res.* **1972**, *32*, 323–325.

(23) Silvestrini, R.; Lenaz, L.; Di Fronzo, G.; Sanfilippo, O. Correlations between cytotoxicity, biochemical effects, drug levels, and therapeutic effectiveness of daunomycin and adriamycin on Sarcoma 180 ascites in mice. *Cancer Res.* **1973**, *33*, 2954–2958.

(24) Wang, J. J.; Chervinsky, D. S.; Rosen, J. M. Comparative biochemical studies of adriamycin and daunomycin in leukemic cells. *Cancer Res.* **1972**, *32*, 511–515.

(25) Gewirtz, D. A. A critical evaluation of the mechanisms of action proposed for the antitumor effects of the anthracycline antibiotics adriamycin and daunorubicin. *Biochem. Pharmacol.* **1999**, *57*, 727–741.

(26) Rivera, E. Liposomal anthracyclines in metastatic breast cancer: clinical update. *Oncologist* **2003**, *8* (Suppl. 2), 3–9.

(27) Shen, F.; Chu, S.; Bence, A. K.; Bailey, B.; Xue, X.; Erickson, P. A.; Montrose, M. H.; Beck, W. T.; Erickson, L. C. Quantitation of doxorubicin uptake, efflux, and modulation of multidrug resistance (MDR) in MDR human cancer cells. *J. Pharmacol. Exp. Ther.* **2008**, *324*, 95–102.

(28) Kalinina, E. V.; Chernov, N. N.; Saprin, A. N.; Kotova, Y. N.; Remizov, V. I.; Shcherbak, N. P. Expression of genes for redox-dependent glutathione *S*-transferase isoforms GSTP1-1 and GSTA4-4 in tumor cell during the development doxorubicin resistance. *Bull. Exp. Biol. Med.* **2007**, *143*, 328–330.

(29) Huet, S.; Robert, J. The reversal of doxorubicin resistance by verapamil is not due to an effect on calcium channels. *Int. J. Cancer* **1988**, *41*, 283–286.

(30) Chauffert, B.; Martin, M.; Hammann, A.; Michel, M. F.; Martin, F. Amiodarone-induced enhancement of doxorubicin and 4′-deoxydoxorubicin cytotoxicity to rat colon cancer cells in vitro and in vivo. *Cancer Res.* **1986**, *46*, 825–830.

(31) van der Graaf, W. T.; de Vries, E. G.; Timmer-Bosscha, H.; Meersma, G. J.; Mesander, G.; Vellenga, E.; Mulder, N. H. Effects of amiodarone, cyclosporin A, and PSC 833 on the cytotoxicity of mitoxantrone, doxorubicin, and vincristine in non-P-glycoprotein human small cell lung cancer cell lines. *Cancer Res.* **1994**, *54*, 5368–5373.

(32) Estevez, M. D.; Wolf, A.; Schramm, U. Effect of PSC 833, verapamil and amiodarone on adriamycin toxicity in cultured rat cardiomyocytes. *Toxicol. in Vitro* **2000**, *14*, 17–23.

(33) Halici, Z.; Dengiz, G. O.; Odabasoglu, F.; Suleyman, H.; Cadirci, E.; Halici, M. Amiodarone has anti-inflammatory and antioxidative properties: an experimental study in rats with carrageenan-induced paw edema. *Eur. J. Pharmacol.* **2007**, *566*, 215–221.

(34) Bates, S. E.; Meadows, B.; Goldspiel, B. R.; Denicoff, A.; Le, T. B.; Tucker, E.; Steinberg, S. M.; Elwood, L. J. A pilot study of amiodarone with infusional doxorubicin or vinblastine in refractory breast cancer. *Cancer Chemother. Pharmacol.* **1995**, *35*, 457–463.

(35) Maeda, H.; Wu, J.; Sawa, T.; Matsumura, Y.; Hori, K. Tumor vascular permeability and the EPR effect in macromolecular therapeutics: a review. *J. Controlled Release* **2000**, *65*, 271–284.

(36) Maeda, H.; Sawa, T.; Konno, T. Mechanism of tumor-targeted delivery of macromolecular drugs, including the EPR effect in solid tumor and clinical overview of the prototype polymeric drug SMANCS. *J. Controlled Release* **2001**, *74*, 47–61.

(37) Ishida, O.; Maruyama, K.; Sasaki, K.; Iwatsuru, M. Size-dependent extravasation and interstitial localization of polyethyleneglycol liposomes in solid tumor-bearing mice. *Int. J. Pharm.* **1999**, *190*, 49–56.

(38) Ranson, M. R.; Carmichael, J.; O'Byrne, K.; Stewart, S.; Smith, D.; Howell, A. Treatment of advanced breast cancer with sterically stabilized liposomal doxorubicin: results of a multicenter phase II trial. *J. Clin. Oncol.* **1997**, *15*, 3185–3191.

(39) Northfelt, D. W.; Dezube, B. J.; Thommes, J. A.; Miller, B. J.; Fischl, M. A.; Friedman-Kien, A.; Kaplan, L. D.; Du Mond, C.; Mamelok, R. D.; Henry, D. H. Pegylated-liposomal doxorubicin versus doxorubicin, bleomycin, and vincristine in the treatment of AIDS-related Kaposi's sarcoma: results of a randomized phase III clinical trial. *J. Clin. Oncol.* **1998**, *16*, 2445–2451.

(40) Gordon, A. N.; Fleagle, J. T.; Guthrie, D.; Parkin, D. E.; Gore, M. E.; Lacave, A. J. Recurrent epithelial ovarian carcinoma: a randomized phase III study of pegylated liposomal doxorubicin versus topotecan. *J. Clin. Oncol.* **2001**, *19*, 3312–3322.

(41) Muggia, F.; Hamilton, A. Phase III data on Caelyx in ovarian cancer. *Eur. J. Cancer* **2001**, *37* (Suppl. 9), S15–S18.

(42) O'Brien, M. E.; Wigler, N.; Inbar, M.; Rosso, R.; Grischke, E.; Santoro, A.; Catane, R.; Kieback, D. G.; Tomczak, P.; Ackland, S. P.; Orlandi, F.; Mellars, L.; Alland, L.; Tendler, C. Reduced cardiotoxicity and comparable efficacy in a phase III trial of pegylated liposomal doxorubicin HCl (Caelyx/Doxil) versus conventional doxorubicin for first-line treatment of metastatic breast cancer. *Ann. Oncol.* **2004**, *15*, 440–449.

(43) Ariga, K.; Kunitake, T. Molecular recognition at air−water and related interfaces: complementary hydrogen bonding and multisite interaction. *Acc. Chem. Res.* **1998**, *31*, 371–378.

(44) Sakai, N.; Matile, S. Anion-mediated transfer of polyarginine across liquid and bilayer membranes. *J. Am. Chem. Soc.* **2003**, *125*, 14348–14356.

(45) Tsogas, I.; Sideratou, Z.; Tsiourvas, D.; Theodossiou, T. A.; Paleos, C. M. Interactive transport of guanidinylated poly(propylene imine)-based dendrimers through liposomal and cellular membranes. *ChemBioChem* **2007**, *8*, 1865–1876.

(46) Tsogas, I.; Theodossiou, T.; Sideratou, Z.; Paleos, C. M.; Collet, H.; Rossi, J. C.; Romestand, B.; Commeyras, A. Interaction and transport of poly(L-lysine) dendrigrafts through liposomal and cellular membranes: the role of generation and surface functionalization. *Biomacromolecules* **2007**, *8*, 3263–3270.

(47) Pantos, A.; Tsiourvas, D.; Sideratou, Z.; Paleos, C. M.; Giatrellis, S.; Nounesis, G. Interactions of complementary PEGylated liposomes and characterization of the resulting aggregates. *Langmuir* **2004**, *20*, 6165–6172.

(48) Pantos, A.; Sideratou, Z.; Paleos, C. M. Complementary liposomes based on phosphatidylcholine: interaction effectiveness vs protective coating. *J. Colloid Interface Sci.* **2002**, *253*, 435–442.

(49) Galanou, M. C.; Theodossiou, T. A.; Tsiourvas, D.; Sideratou, Z.; Paleos, C. M. Interactive transport, subcellular relocation and enhanced phototoxicity of hypericin encapsulated in guanidinylated liposomes via molecular recognition. *Photochem. Photobiol.* **2008**, *84*, 1073–1083.

(50) Olson, F.; Hunt, C. A.; Szoka, F. C.; Vail, W. J.; Papahadjopoulos, D. Preparation of liposomes of defined size distribution by extrusion through polycarbonate membranes. *Biochim. Biophys. Acta* **1979**, *557*, 9–23.

(51) Pantos, A.; Tsiourvas, D.; Paleos, C. M.; Nounesis, G. Enhanced drug transport from unilamellar to multilamellar liposomes induced by molecular recognition of their lipid membranes. *Langmuir* **2005**, *21*, 6696–6702.

(52) Tiberghien, F.; Loor, F. Ranking of P-glycoprotein substrates and inhibitors by a calcein-AM fluorometry screening assay. *Anti-Cancer Drugs* **1996**, *7*, 568–578.

JM800493J